

Ferromagnetic phase transition in zinc blende (Mn,Cr)S-layers grown by molecular beam epitaxy

M. Demper, W. Heimbrod, C. Bradford, K. A. Prior, J. Kehrle, Hans-Albrecht Krug von Nidda, Alois Loidl

Angaben zur Veröffentlichung / Publication details:

Demper, M., W. Heimbrod, C. Bradford, K. A. Prior, J. Kehrle, Hans-Albrecht Krug von Nidda, and Alois Loidl. 2012. "Ferromagnetic phase transition in zinc blende (Mn,Cr)S-layers grown by molecular beam epitaxy." *Applied Physics Letters* 100 (13): 132405. <https://doi.org/10.1063/1.3697834>.



RESEARCH ARTICLE | MARCH 26 2012

Ferromagnetic phase transition in zinc blende (Mn,Cr)S-layers grown by molecular beam epitaxy


M. Demper; W. Heimbrodt; C. Bradford; K. A. Prior; J. Kehrle; H.-A. Krug von Nidda; A. Loidl




Appl. Phys. Lett. 100, 132405 (2012)

<https://doi.org/10.1063/1.3697834>






Lock-in Amplifier



Zurich
Instruments

[Find out more](#)



Boxcar Averager

Boost Your Optics and
Photonics Measurements

Ferromagnetic phase transition in zinc blende (Mn,Cr)S-layers grown by molecular beam epitaxy

M. Demper,¹ W. Heimbrod, ^{1,a)} C. Bradford,² K. A. Prior,² J. Kehrle,³ H.-A. Krug von Nidda,⁴ and A. Loidl⁴

¹Department of Physics and Material Science Center, Philipps University, Marburg 35032, Germany

²Institute of Photonics and Quantum Sciences, SUPA, School of Engineering and Physical Sciences, Heriot-Watt University, Edinburgh EH14 4AS, United Kingdom

³Experimental Physics II, Department of Physics, University of Augsburg, Augsburg 86159, Germany

⁴Experimental Physics V, Center for Electronic Correlations and Magnetism, University of Augsburg, Augsburg 86159, Germany

(Received 23 February 2012; accepted 9 March 2012; published online 26 March 2012)

We studied the magnetization of zinc blende $\text{Mn}_{1-x}\text{Cr}_x\text{S}$ films embedded between diamagnetic ZnSe layers grown by molecular beam epitaxy with chromium mole fractions $x \leq 0.7$. These ternary semiconductors exhibit an increasing ferromagnetic contribution with increasing x caused by competing antiferromagnetic and ferromagnetic coupling. As a result, whereas MnS in the zinc blende phase is a pure antiferromagnet, it was found that with increasing x zinc blende $\text{Mn}_{1-x}\text{Cr}_x\text{S}$ became a ferromagnet. The ferromagnetic phase transition dominates in case of x greater than about 0.5. Hence, we conclude that metastable zinc blende CrS will be a ferromagnetic material with half-metallic character in contrast to the analogous stable NiAs-structure which exhibits an antiferromagnetic phase transition. © 2012 American Institute of Physics. [<http://dx.doi.org/10.1063/1.3697834>]

Half-metallic ferromagnets are discussed as a fundamental ingredient for semiconductor based spintronic devices, because they have a spin alignment at the Fermi energy but an energy gap for the minority spin channel. Based on theoretical calculations Cr-chalcogenides in the zinc blende (ZB) phase have been predicted to be half-metallic ferromagnets.^{1–3} A serious obstacle is the fact that the thermodynamically stable crystallographic phase is the NiAs-structure which exhibits, however, an antiferromagnetic phase transition.⁴ We have shown earlier that growing binary MnS and MnSe on top of zinc blende ZnSe layers stabilizes the metastable ZB phase.^{5,6} In the present paper, we used a similar method to stabilize the ZB structure of ternary (Mn,Cr)S films. The binary end member MnS is an antiferromagnetic semiconductor even in the zinc blende structure. It is the aim of the present paper to study the magnetic properties of (Mn,Cr)S and their respective changes with increasing Cr content.

(Mn,Cr)S/ZnSe heterostructures were grown in a Vacuum Generators V80H MBE System using Zn, Se, Cr, and Mn elemental sources and ZnS to supply sulphur.^{7,8} The structures were grown on GaAs (100) substrates at temperatures of 240–270 °C. All samples were of the form GaAs (sub)/ZnSe (50 nm)/ $\text{Mn}_{1-x}\text{Cr}_x\text{S}$ (d)/ZnSe (50 nm), as we have previously shown that this structure is ideally suited for analysis by x-ray interference (XRI).⁹ This technique provides information on layer thicknesses and compositions for central layers in the nm range.

However, XRI also requires that the (Mn,Cr)S film thicknesses are in the nm-range to avoid exceeding the critical thickness for strain relaxation. The sample details obtained from XRI are given in Table I.

These small layer thicknesses are still sufficient to realize spin manipulation in desired spin devices if the layers

remain ZB. *In situ* RHEED measurements and the high quality of the XRI spectra demonstrate that all the (Mn,Cr)S films exhibit a perfect zinc blende structure. In particular, XRI is sensitive to any perturbation of the crystal structure, such as the presence of dislocations, secondary phases or segregation, and no such effects were observed.

A bright field TEM image is given in Fig. 1 of sample 3 with $x = 0.49$ as an example. The (Mn,Cr)S layer is clearly visible between the ZnSe cladding layers on the GaAs substrate.

The magnetization measurements have been performed in a commercial superconducting quantum interference device (SQUID) magnetometer, Quantum Design MPMS5, in the temperature range $2 \text{ K} \leq T \leq 300 \text{ K}$, where homogeneous fields of -5 to 5 T can be applied. Since there is always a very strong diamagnetic background due to the GaAs substrate and the ZnSe-layers, we sometimes reached the resolution limit of the magnetometer for our thin (Mn,Cr)S-films. Nevertheless, a clear tendency could be revealed, which is seen in Fig. 2. The temperature dependence of the magnetization M is depicted in Fig. 2 for all (Mn,Cr)S-layers at two different external magnetic fields 0.05 T and 0.1 T . The field direction was perpendicular to the growth axis, i.e., in plane.

Despite the fact that the magnetization is rather weak due to the small number of magnetic moments in the layers, significant changes in the magnetization can be observed with increasing x . In Fig. 2(a), the magnetization vs. temperature is depicted for the $\text{Mn}_{1-x}\text{Cr}_x\text{S}$ film with $x = 0.15$. The

TABLE I. Parameters of the $\text{Mn}_{1-x}\text{Cr}_x\text{S}$ -layers.

Sample	1	2	3	4
Cr-content x	≈ 0.15	0.28	0.49	0.68
Layer thickness d (nm)	5 ± 0.5	5 ± 0.5	6 ± 0.5	14 ± 0.5

^{a)}Electronic mail: wolfram.heimbrodt@physik.uni-marburg.de.

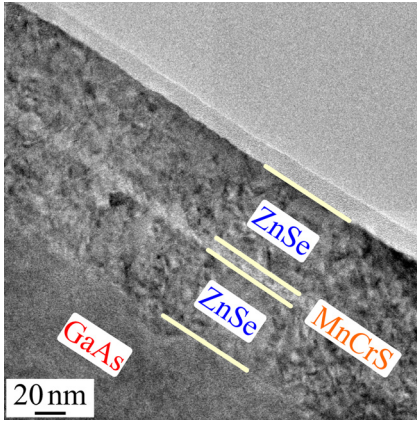


FIG. 1. Bright field TEM image of a ZnSe/Mn_{0.51}Cr_{0.49}S/ZnSe structure on GaAs (sample 3). The (Mn,Cr)S-film thickness is (6 ± 0.5) nm in between (50 ± 4) nm thick ZnSe cladding layers.

curve approximately resembles the curve of pure ZB-MnS with an antiferromagnetic (AF) phase transition and a Néel-temperature of about $T_N = 115$ K.^{10,11} The onset of the AF ordering is seen as kink in the magnetization with decreasing temperatures.

We marked T_N by a dashed line. In Fig. 2(a), T_N is found to be 136 K for the sample with $x \approx 0.15$. At lower temperatures, an additional small ferromagnetic contribution can be seen, which was not observed in pure MnS and is obviously also caused by the Cr incorporation. The onset of this ferromagnetic phase is marked by a dashed-dotted line and is slightly above 50 K.

A similar spectrum but having different transition temperatures was measured for the Mn_{1-x}Cr_xS layer with $x = 0.28$ (Fig. 2(b)). Both phase transition temperatures are now slightly higher compared to Fig. 2(a). The Néel-temperature is about $T_N = 175$ K and $T_C \approx 60$ K.

In terms of a Heisenberg model, the Mn-Mn as well as the Cr-Mn exchange interaction is supposed to be antiferromagnetic, whereas the Cr-Cr interaction should be ferromagnetic.³

In Mn_xCd_{1-x}S, it is known from ESR studies that the Néel-temperature decreases strongly by replacing Mn ions with nonmagnetic cations, which perturbs the magnetic lattice.¹² However, for Mn_xCr_{1-x}S, the Néel-temperature obviously increases which clearly indicates that the AF coupling between Cr and Mn is stronger than the Mn-Mn coupling, i.e., the respective exchange integral is stronger.

Assuming a random distribution (i.e., no ordering or phase separation), the number of Cr ions on the cation sublattice with Cr nearest neighbors also increases with increasing x . Therefore, we suggest the ferromagnetic contribution at low temperatures is caused by the increasing number of Cr-Cr pairs and larger clusters. With increasing mean Cr cluster size, the respective phase transition temperature increases as well. With about $x = 0.5$, the ferromagnetic coupling becomes dominant.

In Figs. 2(c) and 2(d), the magnetization curves are depicted for $x = 0.49$ and 0.68 , respectively. The magnetization is now clearly dominated by the ferromagnetic phase transition and no antiferromagnetic phase transition can be seen anymore. The Curie-temperatures are $T_C \approx 90$ K for $x = 0.49$ and $T_C \approx 114$ K for $x = 0.68$, respectively. We can conclude, therefore, that the changes of the magnetic behavior are correlated with x , in particular, the ferromagnetic contribution increases and the respective Curie-temperatures shift significantly to higher temperatures with increasing x .

Fig. 3 shows a summary of these data as a function of x . We found no significant difference for the two field strengths and therefore the mean values are depicted for (Mn,Cr)S. The additional values for $x = 0$ are taken from earlier measurements on MBE grown MnS-Films with a thickness of

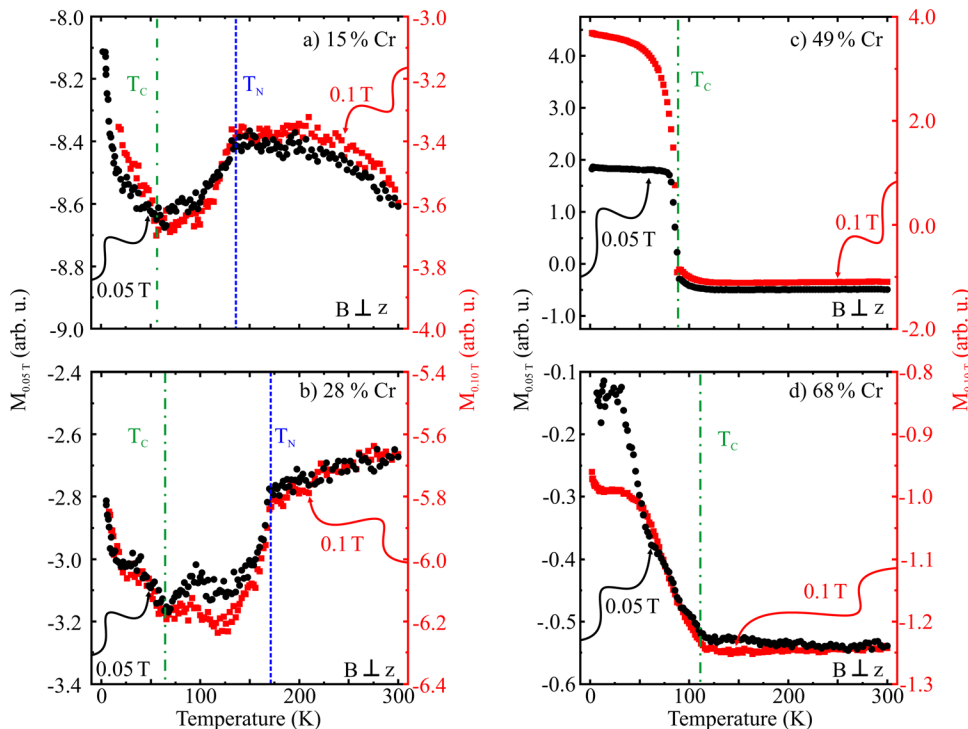


FIG. 2. Magnetization data of the Mn_{1-x}Cr_xS films in different external magnetic fields of 0.05 T and 0.1 T. (a) Sample 1, $x = 0.15$. (b) Sample 2, $x = 0.28$. (c) Sample 3, $x = 0.49$. (d) Sample 4, $x = 0.68$.

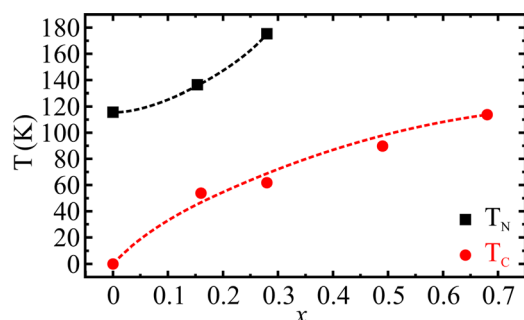


FIG. 3. Magnetic phase transition temperatures of metastable zinc blende $\text{Mn}_{1-x}\text{Cr}_x\text{S}$ films between ZnSe cladding layers as a function of x . Red points: Curie-temperature T_c ; black squares: Néel-temperature T_N .

8.3 nm.¹³ For both transition temperatures, T_N and T_c , a significant increase can be seen. While the Néel-temperature T_N was observed only for $x < 0.28$, the Curie-temperature T_c is observable over the entire concentration range and reaches $T_c = 115$ K for $x = 0.68$.

It should be noted that at large x the coexistence of the two competing magnetic phases disappears and the magnetization is dominated by the ferromagnetic component only. In other words, by incorporating chromium into the antiferromagnetic ZB MnS it is possible to obtain a ferromagnetic semiconductor. Therefore, we have demonstrated experimentally that in $(\text{Mn,Cr})\text{S}$ the Cr-Cr exchange coupling mediated by S anions is obviously ferromagnetic in the ZB structure. We expect, therefore, on the basis of our experimental findings that ZB CrS should also be a ferromagnetic material and might have the expected half-metallic character. Thus, the metastable zinc blende CrS phase would be fundamentally different to the well known CrS in the thermodynamically stable NiAs-structure which is an antiferromagnet.

Long *et al.*³ calculated the influence of the incorporation of different transition metals such as chromium or vanadium into zinc blende Mn chalcogenides. From calculations of the density of states and the magnetic properties, it was found that the incorporation of Cr or V leads to a half-metallic character and introduces a ferrimagnetic phase. The latter is a result of the competing magnetic couplings of the ferro-

magnetic Cr-Cr and the antiferromagnetic Cr-Mn and Mn-Mn interactions. From this, Long *et al.* explained an increase of the ferrimagnetic transition temperature. For chromium concentrations in the range $0 \leq x \leq 0.3$, they calculated a shift of the transition temperature up to 500 K. We could not find convincing evidence for ferrimagnetism and our ferromagnetic phase transition temperatures are considerably smaller. However, mean field calculations usually overestimate phase transition temperatures.

In summary, it was found that ZB $(\text{Mn,Cr})\text{S}$ layers with $x < 0.3$ exhibit both an antiferromagnetic and a ferromagnetic phase transition driven by the coexistence of antiferromagnetic Mn-Mn and Mn-Cr coupling and ferromagnetic Cr-Cr coupling. Above $x = 0.5$, the ferromagnetic coupling becomes the dominant mechanism and MnCrS behaves like a ferromagnet.

The authors acknowledge the support by EPSRC and the German Research Foundation (EGC 790 Electron-Electron Interaction in Solids, TRR 80—From Electronic Correlations to Functionality) and are grateful to Dana Vieweg for performing the magnetic measurements.

¹W.-H. Xie, Y.-Q. Xu, B.-G. Liu, and D. G. Pettifor, *Phys. Rev. Lett.* **91**, 037204 (2003).

²K. Yao, G. Gao, Z. Liu, and L. Zhu, *Solid State Commun.* **133**, 301 (2005).

³N. H. Long, M. Ogura, and H. Akai, *J. Appl. Phys.* **106**, 123905 (2009).

⁴G. I. Makovetskii and G. M. Shakhlevich, *Phys. Status Solidi A* **47**, 219 (1978).

⁵M. Demper, L. Chen, C. Bradford, K. Prior, and W. Heimbrodt, *Solid State Commun.* **150**, 1092 (2010).

⁶M. Demper, W. Heimbrodt, C. Bradford, and K. Prior, *J. Nanopart. Res.* **13**, 5635 (2011).

⁷L. David, C. Bradford, X. Tang, T. Graham, K. A. Prior, and B. C. Cavenett, *J. Cryst. Growth* **251**, 591 (2003).

⁸K. A. Prior, C. Bradford, L. David, X. Tang, and B. C. Cavenett, *Phys. Status Solidi B* **241**, 463 (2004).

⁹K. Prior, X. Tang, C. O'Donnell, C. Bradford, L. David, and B. Cavenett, *J. Cryst. Growth* **251**, 565 (2003).

¹⁰W. S. Carter, *Proc. Phys. Soc.* **76**, 969 (1960).

¹¹O. Goede and W. Heimbrodt, *Phys. Status Solidi B* **146**, 11 (1988).

¹²O. Goede, D. Backs, W. Heimbrodt, and M. Kanis, *Phys. Status Solidi B* **151**, 311 (1989).

¹³M. Demper, L. Chen, H.-A. Krug von Nidda, C. Bradford, A. Loidl, K. A. Prior, and W. Heimbrodt, *Phys. Status Solidi C* **7**, 1636 (2010).